

## **General Disclaimer**

### **One or more of the Following Statements may affect this Document**

- This document has been reproduced from the best copy furnished by the organizational source. It is being released in the interest of making available as much information as possible.
- This document may contain data, which exceeds the sheet parameters. It was furnished in this condition by the organizational source and is the best copy available.
- This document may contain tone-on-tone or color graphs, charts and/or pictures, which have been reproduced in black and white.
- This document is paginated as submitted by the original source.
- Portions of this document are not fully legible due to the historical nature of some of the material. However, it is the best reproduction available from the original submission.

NATIONAL AERONAUTICS AND SPACE ADMINISTRATION

*Technical Memorandum 33-743*

*Silicon Crystal as a Low Work Function  
Collector*

*K. H. Chang*

*K. Shimada*

(NASA-CR-145791) SILICON CRYSTAL AS A LOW  
WORK FUNCTION COLLECTOR (Jet Propulsion  
Lab.) 16 P HC \$3.50 CSCI 20B

N76-12857

Unclas

G3/76 03738

JET PROPULSION LABORATORY  
CALIFORNIA INSTITUTE OF TECHNOLOGY  
PASADENA, CALIFORNIA

October 15, 1975



NATIONAL AERONAUTICS AND SPACE ADMINISTRATION

*Technical Memorandum 33-743*

*Silicon Crystal as a Low Work Function  
Collector*

*K. H. Chang*

*K. Shimada*

JET PROPULSION LABORATORY  
CALIFORNIA INSTITUTE OF TECHNOLOGY  
PASADENA, CALIFORNIA

October 15, 1975

## PREFACE

The work described in this report was performed by the Guidance and Control Division of the Jet Propulsion Laboratory.

## CONTENTS

I. Introduction . . . . .	1
II. Test Vehicle and Experimental Techniques . . . . .	2
III. Results . . . . .	4
IV. Discussion of Results . . . . .	5
V. Conclusions . . . . .	8
References . . . . .	8

### TABLE

1. Performance Comparison of High and Low Temperature Thermionic Converter . . . . .	9
--	---

### FIGURES

1. Schematic of the Test Vehicle . . . . .	10
2. Test Set Up Photograph . . . . .	11
3. Collector Assembly . . . . .	12
4. Photoemission During Activation . . . . .	13
5. I-V Characteristic with Photoemission Current . . . . .	13
6. Quantum Efficiency vs. Photon Energy . . . . .	14
7. Raser-Warner Plot of Si . . . . .	14
8. Thermionic Emission vs. Emitted Voltages . . . . .	15
9. Effective Cesium Temperature, $T_{Cs}$ vs. Reservoir Temperature, $T_R$ . . . . .	15

PRECEDING PAGE BLANK NOT FILMED

## ABSTRACT

For the purpose of developing a low work function collector which can be incorporated in a thermionic converter, a test vehicle with the collector assembly was constructed from standard vacuum components including an ultra-high vacuum ion pump. The collector assembly was fabricated by diffusion bonding a (100) oriented silicon single crystal to a molybdenum block. The silicon surface was treated with cesium and oxygen to produce an NEA-type condition and the results were tested by photoemission and work function measurements.

An n-type silicon collector was successfully activated to a work function of 1.0 eV, which was verified by photoemission spectral yield measurements. The stability test of an activated surface at elevated temperatures was conducted in the range from room temperature to 619°K, which was slightly lower than the designed collector temperature of 700°K. The work function measurements clearly demonstrated that the behavior of cesium replenishment on the activated Si surface was similar in nature to that of a metallic surface; that is, the loss of cesium by thermal desorption could be compensated by maintaining an adequate vapor pressure of cesium.

## I. INTRODUCTION

Analyses of current state-of-the-art thermionic converters have indicated<sup>(1)</sup> that further improvements in conversion efficiencies of thermionic diode converters must arise from a decrease in collector work function and a reduction of the plasma voltage drop. The two phenomena are not totally independent of each other, but in large part, the problems can be separated.

The problem of reducing the surface work function has been extensively pursued for improving photo-electron emitters, and values lower than 1.0 electron volts have been achieved in a number of metal-oxide-cesium systems<sup>(2)</sup> and semiconductor-cesium-oxygen systems<sup>(3,4)</sup>. However, existing collectors usually exhibit a work function larger than 1.5 eV<sup>(1)</sup> in thermionic converters.

Therefore, during the past few years, research has been in progress to develop a low work function collector which would be usable in low-temperature thermionic converters. If one can achieve a barrier index (sum of the collector work function and the plasma drop) of 1.2 eV, a conversion efficiency at the electrodes as high as 29% can be achieved at an emitter temperature  $T_E$  of 1400°K (see Table 1).

The purpose of the present study is to develop a low work function collector, less than 1.2 eV, by adopting the techniques developed for photocathode materials. Among a few potential candidate materials such as metal-oxide-cesium and semiconductor cesium-oxygen systems, (100) oriented silicon single crystal was chosen as the collector material for further investigation. A silicon (100) surface has already been successfully activated to  $\phi \leq 1.0$  eV and has been tested at elevated temperatures<sup>(5)</sup> elsewhere. A similar collector was incorporated in a simulated thermionic converter at JPL in which measurement of work function and the diode characteristics were performed.

The details of the experimental procedures and the results from one n-type silicon electrode are presented in this paper.

## II. TEST VEHICLE AND EXPERIMENTAL TECHNIQUES

### Test Vehicle

A schematic drawing of the test vehicle is shown in Figure 1. The envelope is made of a standard vacuum component, a 38-mm (1.5-inch) stainless steel "cross". A pair of opposite ports of the cross are used for the emitter and collector mounting, the remaining two ports are used for the vacuum pump connection and an observation window. Two small tubes are welded at a 45° angle to the wall of the cross in order to provide a port for another optical window and a port with a valve for the cesium supply. In addition, oxygen and argon supply lines are incorporated through a double flange at the observation window. The external view of the actual test system is shown in Figure 2.

The emitter is made of a 90% transparent 100-mesh tungsten sheet screen (25  $\mu$ m (0.001") thick). An identical mesh, separated by 1.6mm is provided so that it may be used as a grid electrode. The emitter is directly heated by a 60 Hz AC power supply. The reason for the emitter being a transparent screen is that the collector surface must be in a line of sight from the optical window and the cesium tube for the photoemission measurements and for the cesiation by the cesium beam.

The collector assembly (Fig. 3) is made of a 0.25mm thick silicon wafer bonded on a molybdenum block, and this assembly is surrounded by a guard ring. The Si-Mo bonding was performed by heating them together in vacuum to about 1100°C. The bonding temperature was below the Si-Mo eutectic point (1400°C) and the Si surface visually maintained its original appearance after the bonding. The stress due to the thermal expansion mismatch causes the bond to break unless the rate of temperature variation is maintained at 10°C per minute or less.

The cesium source is connected to the main chamber through a stainless steel valve. The valve is open only during the period of cesiation. A temperature controlled heater is wrapped around the reservoir to control the cesium flux arriving at the Si electrode surface.

Reagent grade oxygen and argon sources are also incorporated in the test system. Oxygen is used as an activating agent for the test electrode; argon is used as the source of ions for sputter cleaning. These gases are contained



in two glass flasks at one atmosphere pressure and are introduced to the system via precision flow control valves. The valve for the oxygen is a variable leak valve by Varian Associates (minimum leak rate  $(1.3 \times 10^{-8} \text{ N/m}^2\text{-l/sec})$  ( $1 \times 10^{-10} \text{ Torr-liter/sec}$ )). The valve for argon is a micrometer controlled needle valve.

An absorption pump is provided for roughing the test vehicle, and a 200 l/s ion pump is used to attain ultrahigh vacuum ( $10^{-7} \text{ N/m}^2$  ( $10^{-9} \text{ Torr}$ )). The pressure in the test chamber is estimated by reading the ion pump current.

### Experimental Techniques

Si-Mo Bonding. A single crystal wafer of silicon was diffusion bonded on a molybdenum substrate without destroying the crystallinity of silicon. The silicon wafer was first boiled in acetone, then cleaned in HF prior to the final rinse in DI water. The molybdenum was carefully machined to insure its surface flatness and electro-chemically cleaned prior to assembly. To bond the two pieces they were heated in a diffusion-pumped vacuum system ( $p = 1.3 \times 10^{-4} \text{ N/m}^2$  ( $10^{-6} \text{ Torr}$ )) to 1100-1200°C by electron bombardment of the molybdenum block. The bonding initiated at one point, which became brighter than the rest of the silicon surface, and the bright area increased as the bonding spread over the entire surface in about 15 minutes. A slight pressure of about  $1 \text{ N/cm}^2$  was helpful in initiating the bond. To achieve a successful bonding the cooling rate must be less than 10°C per minute.

Activation. The activation procedure which has been published in the literature<sup>(6)</sup> was followed in this experiment. The silicon surface was first cleaned in the vacuum system by argon ion bombardment ( $1 \text{ mA/cm}^2$ , 15 min at 950 volts) and subsequently annealed at 1000°C for about an hour. When the silicon was cooled to room temperature, cesium was administered on its surface while photoemission was monitored. The surface was first overcesiated (more than one monolayer coverage) and oxygen was added afterward to complete the activation. The degree of activation was monitored by measuring the photoemission current (Fig. 4).

Photoemission Measurements. The light source for the measurement was a 100 watt quartz-iodine tungsten lamp. The image of an appropriate aperture was made to focus on the specimen through quartz lenses. A series of interference filters with approximately 10 nm pass band are used to measure the spectral

response. Since the entire area of the specimen is illuminated, the results are the average values over the area. From these measurements the surface work function was determined.

Work Function Measurements. The work function of the activated surface was also measured by the retarding potential method. In this method, photoemission current was generated from the activated surface by illuminating it with white light. The photo-emitted electrons are collected by the tungsten screen emitter. By measuring the voltage at the saturation current 'knee' in the I-V curve, the work function difference of the two electrodes was established (Fig. 5). If the work function of one electrode is known, the work function of the other is determined as well. In this experiment, the work function of the cesiated tungsten surface was determined by measuring its spectral photoemission threshold, and it provided the necessary reference work function. Ordinarily the thermionic emission from the emitter was used as the electron source for the retarding potential method, but for this experiment, the glowing emitter induced photoemission from the activated collector which interfered with the emitter thermionic current. Therefore the photoemission, resulting from an external light source, was used as the electron source in place of the thermionic emission.

Temperature Measurements. The temperature of the collector was measured by a tungsten-Rhenium thermocouple up to approximately 800°C and an optical pyrometer was used at higher temperatures. The collector heating was accomplished by electron bombardment using a tungsten wire loop located inside the guard ring.

### III. RESULTS

The activation was performed with an n-type crystal having a (100) surface. The activation reduced the work function of the Si surface to 1.0 eV as measured by the I-V curve (Fig. 5) and the spectral photoemission measurements (Fig. 6).

The stability of the activated surface was tested in the range from room temperature to 620°K. The result was plotted in a Rasor-Warner plot as shown in Fig. 7. The temperature measurements were not accurate as will be mentioned in the discussion; therefore the results should be considered

preliminary. However, the behavior of the activated silicon surface clearly indicates that it follows the same trend as that of a metal surface in contact with cesium vapor.

#### IV. DISCUSSION OF RESULTS

##### Activation

A diffusion bonding technique was developed in which no bonding agent was applied, allowing the annealing temperature to reach 1000°C after the bonding. Such a temperature is required to achieve a successful activation, and this temperature cannot be reached if brazing is employed for bonding of Si to Mo. An n-type sample mounted by the diffusion bonding technique was successfully activated to a work function of 1.0 eV, which was confirmed by both the I-V curve (Fig. 5) and the photoemission spectral response measurements (Fig. 6). It is noted in Fig. 4 that the addition of oxygen at the end of cesiation increased the white light photoemission, but the increase was only 30%, while the reported<sup>(6)</sup> increase on p-type sample is by a factor of about 10. This small increase in our experiment is due to the fact that the sample is n-type silicon in which the band bending is not favorable for electron emission. One would expect that the white light photoresponse from an n-type Si increases only marginally at work functions below about 1.4 eV while the white light response from a p-type makes a large increase at an instant when the NEA condition is achieved. It was also noted that when the cesiated surface did not receive an oxygen treatment the stability of the surface was very poor and the photoemission would decrease to about 10% of original value in 10-20 minutes. When the oxygen treatment was given, the surface would maintain its low work function for a few days without an appreciable degradation in photoemission.

##### I-V Characteristics

The I-V characteristics of the simulated converter are shown in Fig. 8. The curve No. 1 is for the collector before activation and the curve No. 2 after activation. When the collector was activated to attain its work function of 1.0 eV, the level of photoemission due to the bright light from the hot emitter was approximately in the same order of magnitude ( $10^{-8}$  ampere). Therefore the measured current was biased by this photoemission current.

The curve No. 2 was obtained by shifting it vertically upward so that the bottom line coincided with the zero line of the current axis, in an attempt to determine the change of work functions. However, a quantitative measurement of work function was impossible from these I-V curves because of the change in shape of the curve.

Therefore the photoemission current from the collector was used as the current source in obtaining I-V characteristics. The emitter was cooled and used as the collector of this current. This method, in fact, produced sharp knees whose positions were easily identifiable (Fig. 5). From the position of the knee in the figure one can determine the true work function difference of two electrodes under consideration; hence, it is imperative to accurately determine, by an independent method, the work function of one of the two surfaces. A grid electrode (tungsten mesh, identical to the emitter), which was fully cesiated, was suitable for this purpose. The work function of the grid electrode was low enough so that the spectral response of photoemission was measurable and the work function of the grid was accurately determined to be 1.65 eV. The point marked "a" in Fig. 5 indicates the knee from which the collector work function of 1.0 eV is derived (see the insert in the figure). The point marked "b" provides an additional verification. If the collector work function is assumed to be 1.0 eV, the bare work function of the emitter electrode is 4.65 eV. In view of the fact that the emitter, which was flash-cleaned, was polycrystalline tungsten and that the surface could be covered with a thin oxide layer, the value 4.65 eV is very reasonable. These work function values are considered accurate within about 0.05 eV. The uncertainty arises from the uncertainty in determining the precise position of the "knee." The photoemission spectral response measurement of the activated collector surface (Fig. 6) shows a threshold at approximately 1.0 eV, which is another verification independent of the I-V curves.

#### Temperature Stability

The results of the work function measurements at elevated temperature are as shown in Fig. 7. In this figure,  $T_{Cs}$  was calculated from the cesium beam arrival rate. The temperature measurements for this experiment were not accurate because the silicon electrode became detached at this phase of the experiment. Consequently, error-bars are shown to define the region of confidence for each data point. However, the results clearly demonstrated

that the behavior of cesium replenishments on the activated silicon surface were similar in nature to that of the metallic surface; that is, the loss of cesium by thermal desorption could be compensated by maintaining an adequate vapor pressure of metallic cesium. This is in contrast with the published result of Goldstein<sup>(5)</sup>, who reported no loss of cesium up to the temperature of 700°K and no loss of oxygen up to nearly 1100°K. The discrepancy may be attributed to the fact that his results were obtained in non-equilibrium conditions whereas our results were obtained in quasi-equilibrium conditions. The collector surface temperature was estimated from the temperature measurement of the molybdenum block. Since the silicon wafer became detached at the time of this experiment, temperature of the silicon wafer was estimated by allowing a temperature drop of 20% in °C across the molybdenum block and the crystal. The choice of 20% was based upon many observations during the diffusion bonding experiments.

The Cs vapor flux on the Si surface is controlled by the temperature of the Cs reservoir. The reservoir, however, is located about 25 cm away from the collector surface and an isolating valve is located in the path of the Cs vapor. Therefore the arrival rate of Cs vapor onto the collector surface is not the value determined by the reservoir temperature but is much lower. Considering the molecular flow through the connecting tube and the transmission coefficient of the two tungsten meshes (emitter and grid) the Cs arrival rate was calculated to be 1% of the cesium evaporation rate at the liquid cesium surface. The calculated Cs temperature  $T_{Cs}$  as a function of  $T_R$  is shown in the top curve of Fig. 9. The bottom curve shows the effective reservoir temperature obtained from the activation time measurements. The photo response data, (Fig. 4) indicated that approximately one monolayer coverage of Cs occurred at approximately 5-10 minutes. Assuming the sticking coefficient of Cs molecules to be unity at submonolayer coverages, and correlating the atomic impinging rate with the cesium vapor pressure, an effective pressure of cesium was deduced. Impinging rate, which was calculated from the activation time measurements, was 0.1% of the cesium evaporation rate of the liquid cesium due to the separation of the Cs reservoir and the collector surface. The horizontal error bars in Fig. 7 were generated from these two lines in Fig. 9.

## V. CONCLUSIONS

A collector work function of 1.0 eV has been achieved in a simulated thermionic converter by using an n-type silicon which is diffusion bonded to a molybdenum block as the collector.

The collector work function vs. its temperature measurements clearly demonstrated that the behavior of cesium replenishment on the activated Si surface is similar in nature to that on metallic surface; that is, the loss of cesium by thermal desorption can be compensated by maintaining an adequate vapor pressure of metallic cesium.

### Acknowledgements

Authors acknowledge Mr. Michael Donovan for his contributions in achieving a successful Si-Mo bonding.

### References

1. N. S. Rasor (1972), Proceedings of Third International Conference on Thermionic Electric Power Generation, Juelich, P. 1027, June 59.
2. V. S. Fomenko (1966), Edited by G. V. Samsonov, Handbook of Thermionic Properties, Plenum Press Data Division.
3. Alleau, T. and Eacal, M. (1970), Report of Thermionic Conversion Specialist Conf., P. 434, Miami, Fla.
4. A. H. Sommer (1968), "Photoemissive Materials, Preparation, Properties and Uses," Wiley, New York.
5. Bernard Goldstein (1973), "LEED, Auger and Plasmon Studies of Negative Electron Affinity on Si produced by the Adsorption of Cs and O." Surf. Sci. 35 227.
6. R. U. Martinelli (1973), Journal of Appl. Phys. Vol. 44, 2566.

Table 1. Performance Comparison of High and Low  
Temperature Thermionic Converter

Variables			High Temp. Conv.	Low Temp. Conv.	
				Advanced	Ideal
Emitter Temp.,	$T_E$	(K)	2000	1400	1400
Collector Temp.,	$T_C$	(K)	1000	700	700
Cesium Temp.,	$T_{CS}$	(K)	600	400	400
Emitter Work Function,	$\phi_E$	(eV)	3.0	2.0	2.0
Collector Work Function,	$\phi_C$	(eV)	1.7	1.0	1.0
Plasma Drop,	$V_P$	(V)	0.6	0.2	0
Output Volt.,	$V_O$	(V)	0.7	0.8	1.0
Output Current,	$I_O$	(A/cm <sup>2</sup> )	12	14	14
Output Power,	$P_{OUT}$	(W/cm <sup>2</sup> )	8.4	11	14
Input Power,	$P_{IN}$	(W/cm <sup>2</sup> )	70	40	40
Efficiency,	$\eta$	(%)	12	29	35

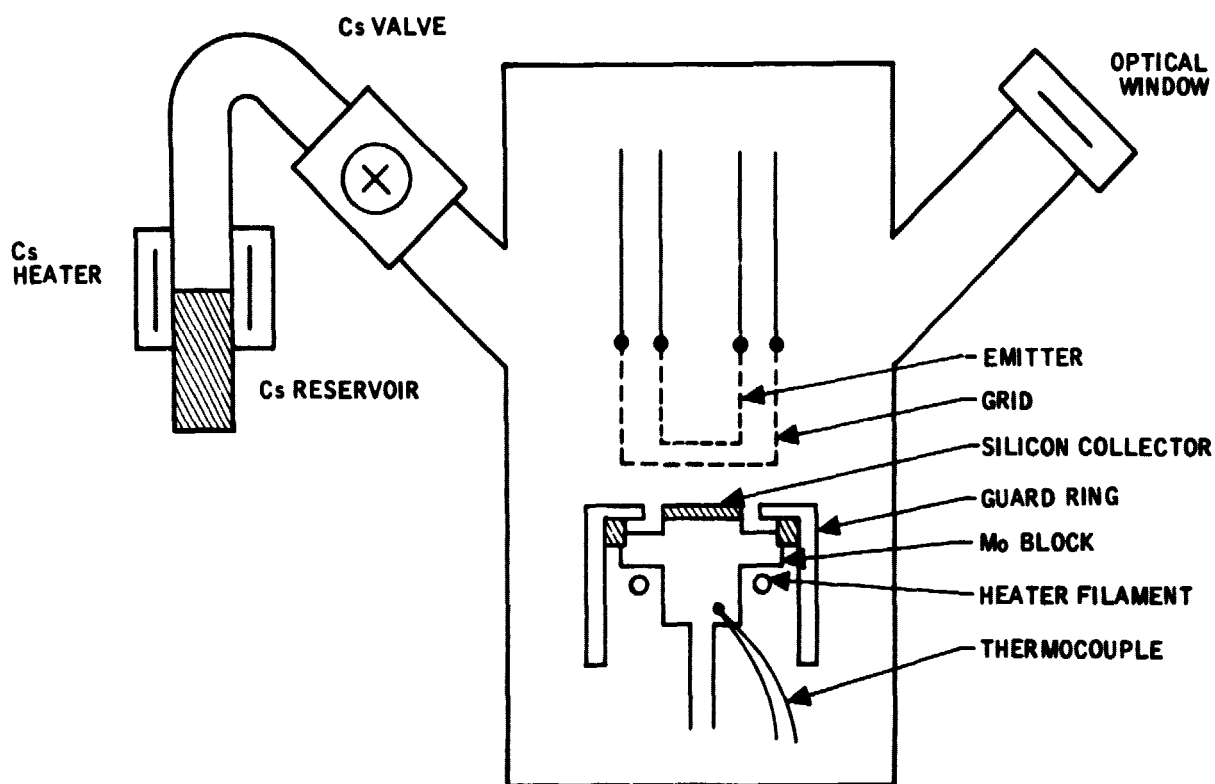


Fig. 1. Schematic of the test vehicle



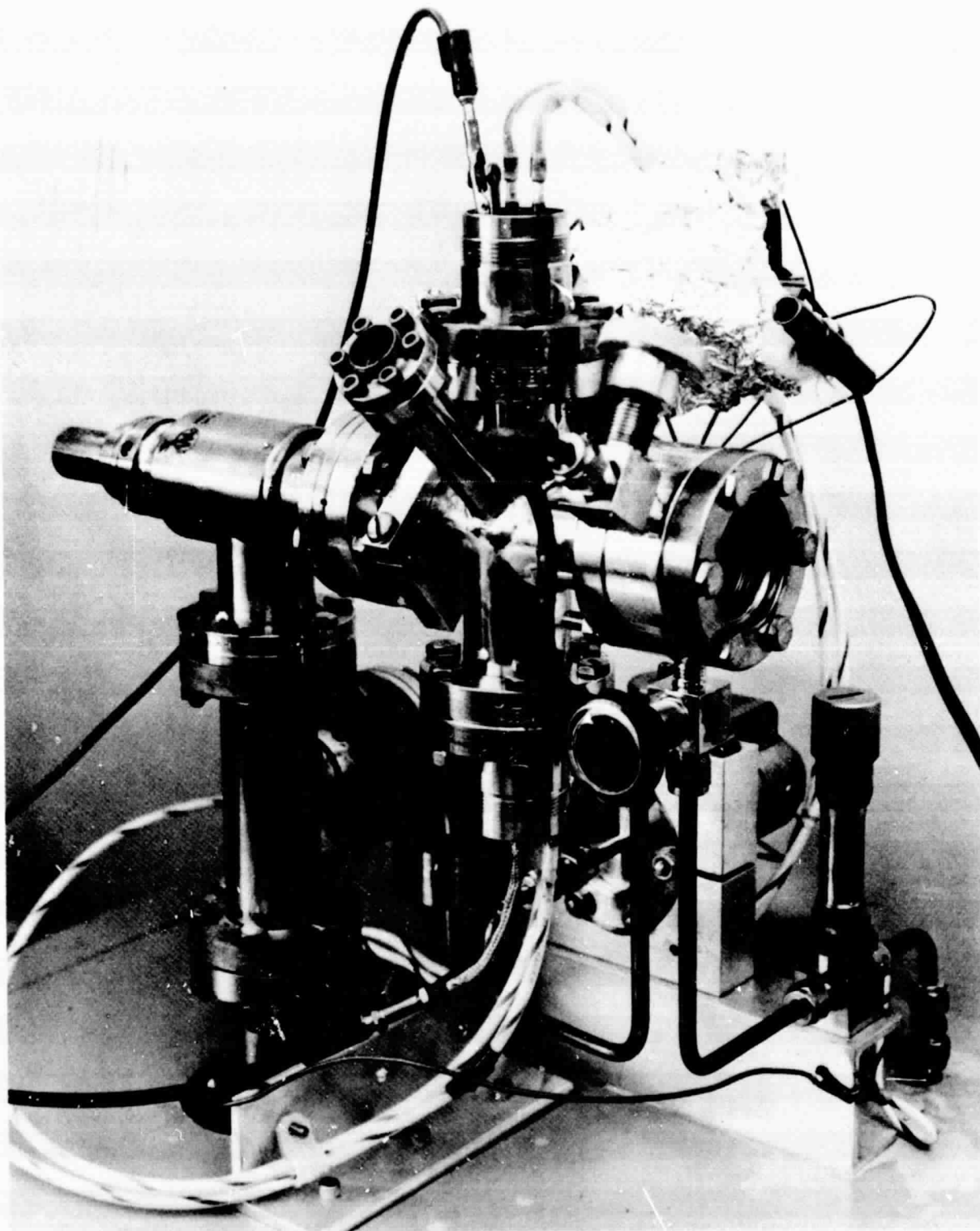


Fig. 2. Test set up photograph

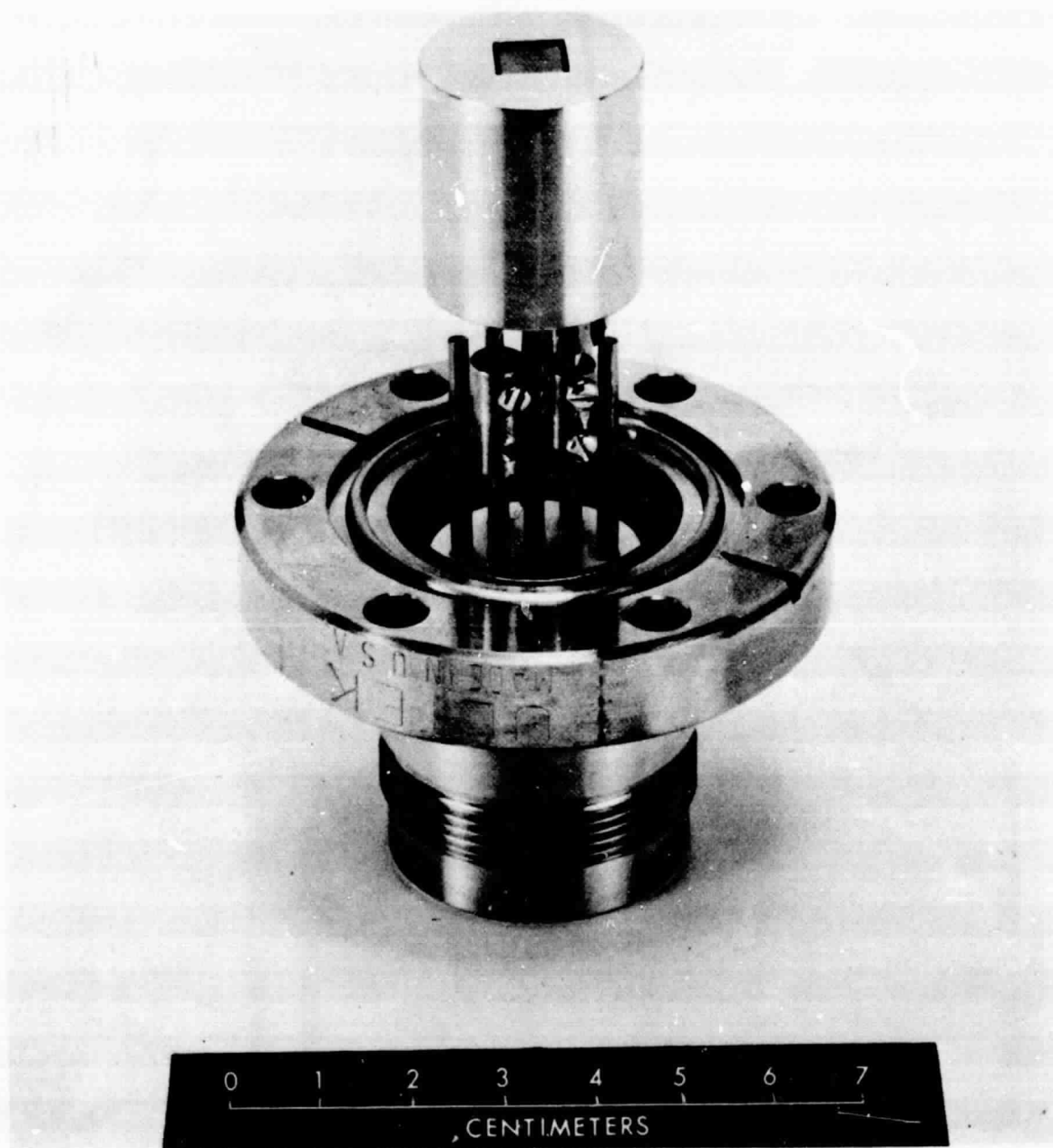


Fig. 3. Collector assembly

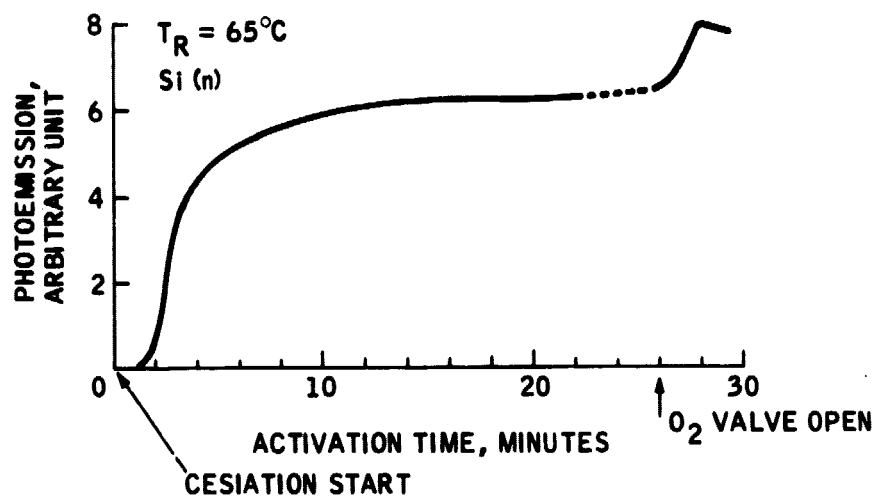
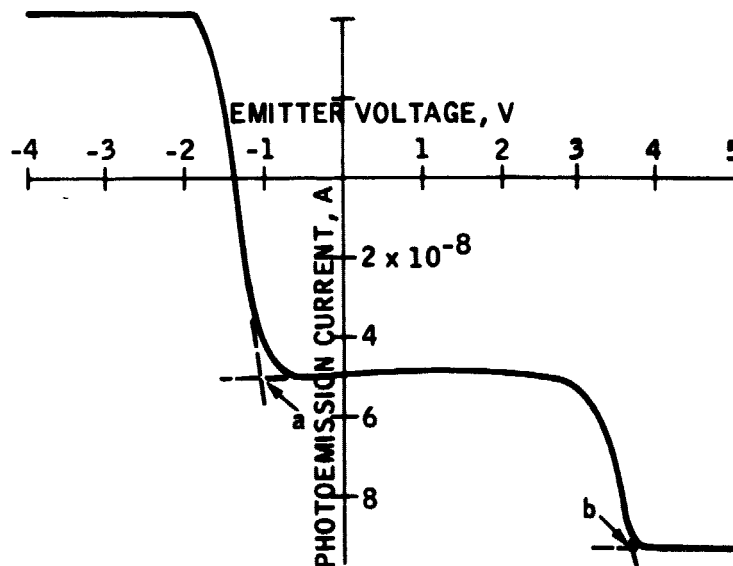


Fig. 4. Photoemission during activation



POINT (a)  
 $\phi_g = 1.65$   
 $V_g = -1.75$   
 $\phi_c = (\phi_g + V_g) - V$   
 $\phi_c = 1.0$   
 $V = -1.1$

POINT (b)  
 $\phi_c = 1.0$   
 $V = 3.65$   
 $\phi_E = 4.65$   
 $\phi_c = \phi_E - V$

Fig. 5. I-V characteristic with photoemission current

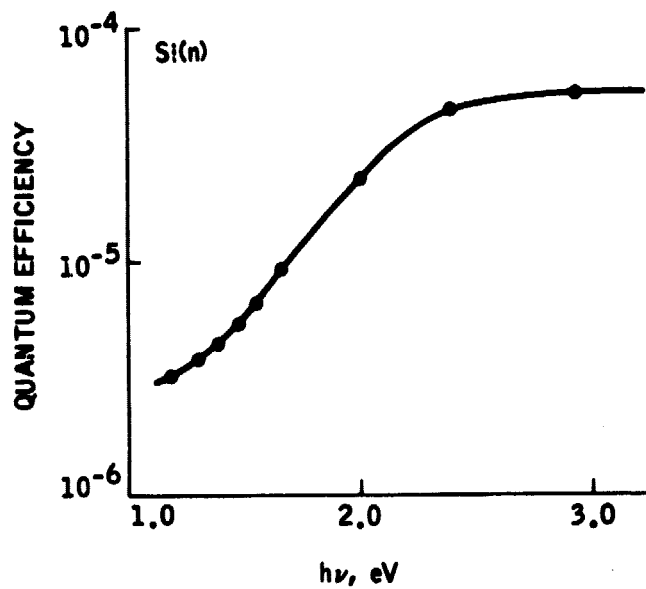


Fig. 6. Quantum efficiency vs. photon energy

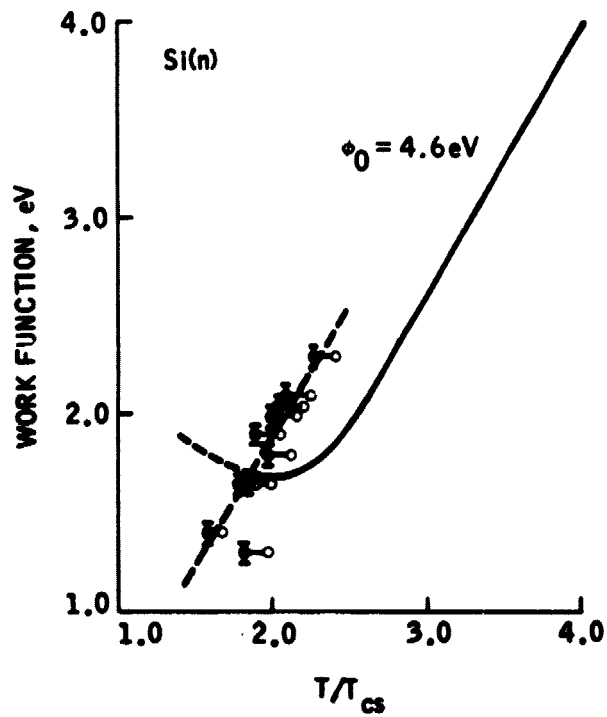


Fig. 7. Raser-Warner plot of Si

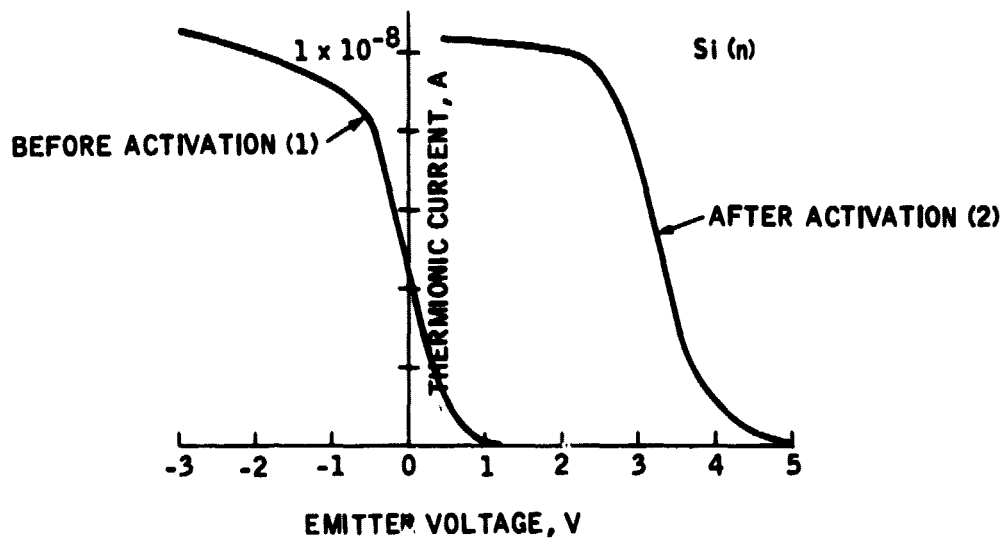


Fig. 8. Thermionic emission vs. emitted voltages

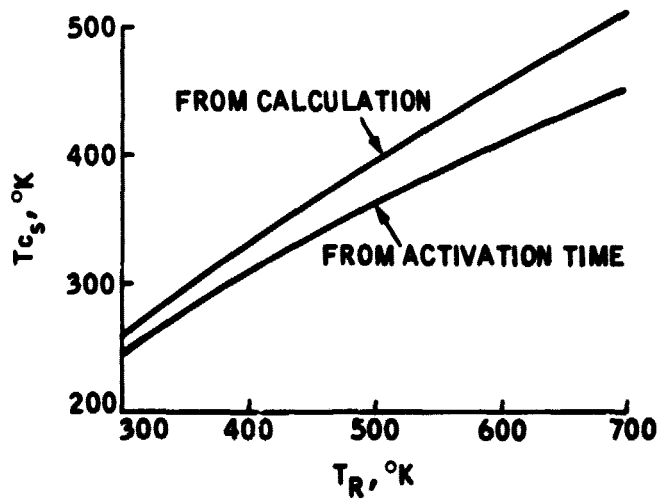


Fig. 9. Effective cesium temperature,  $T_{Cs}$  vs. reservoir temperature,  $T_R$